Influence of the growth technique on the coupling and magnetoresistance of Co/Ru sandwiches

S. Zoll, A. Dinia,* J. P. Jay, C. Mény, G. Z. Pan, A. Michel, L. El Chahal, V. Pierron-Bohnes, and P. Panissod
IPCMS-GEMME (UMR 46 du CNRS), 23 rue du Loess, F-67037 Strasbourg, France

H. A. M. Van den Berg
Siemens AG, ZFE T MR 1, P.O. Box 3220, D-91050 Erlangen, Germany
(Received 25 July 1997)

A comparative study of the structure and magnetotransport properties of Co/Ru sandwiches grown by evaporation in ultrahigh vacuum (UHV) and by plasma sputtering is reported. The crystalline structure of both types of samples has been studied by x-ray diffraction and transmission electron microscopy and the interfacial morphology by nuclear magnetic resonance. The comparison shows that the main structural difference comes from the crystalline quality: the evaporated samples are single crystals whereas the sputtered samples are polycrystalline and not textured. This difference in structure has no significant effect on the magnetoresistance, which is small for both growth techniques and is attributed to the strong interfacial mixing observed in both cases. The crystalline quality has a stronger effect on the exchange coupling. Indeed, its strength is more than a factor of 2 larger in the UHV samples than in the sputtered ones. Moreover, we observe that the shape of the room-temperature coupling oscillations obtained with the UHV samples is in good agreement with *ab initio* calculations. This indicates that the coupling is very homogeneous in those samples. Surprisingly the agreement is still good at low Ru thicknesses where ferromagnetic bridges are usually observed. This has been studied in more detail by temperature-dependent magnetometry. It shows that the absence of ferromagnetic bridges is due to the interfacial magnetization reduction (a consequence of the interfacial mixing), which prevents, at room temperature only, the appearance of ferromagnetic bridges. [S0163-1829(98)03208-1]

I. INTRODUCTION

Thin films composed of alternating layers of magnetic and nonmagnetic metals have found growing interest and a range of applications in the past ten years.[1] For a large number of combinations of metals, an oscillatory ferromagnetic-antiferromagnetic (AF) indirect exchange coupling appears between the magnetic layers through the nonmagnetic layer[2] and sometimes a giant magnetoresistance (GMR) effect[3] which is not necessarily correlated to this exchange coupling. In particular, Fe/Cr,[4] Co/Cu,[5,6] Co/Au,[7] Co/Ag,[8] and Co/Ru (Ref. 2) systems have been extensively studied. A large number of theoretical studies have been done in order to explain the origin of the exchange coupling in these multilayers. The recent theories[9] mostly describe it by using the quantum interferences originating from the electron confinement in the spacer layer and show the importance of the morphology of the interfaces on the strength of the coupling and on its evolution with the thickness of the spacer.

The Co/Ru system has been already studied by different authors[2,10,11] and presents some interesting particularities. The coupling appears to be very sensitive to the preparation conditions and the GMR is always quite small, whereas Campbell and Fert[12] predicted that the GMR should be high in this system, on the basis of the resistivity change expected from Ru impurities diluted in a Co matrix.

Since the magnetic and transport properties of Co/Ru multilayers are very sensitive to the growth conditions, it is interesting to know if the main effect lies in the shape of the interfaces or in the crystalline quality. Hence, the aim of this work is to compare the structure, the magnetic and transport properties of samples with the same geometry, grown by ultrahigh vacuum (UHV) molecular beam evaporation and by sputtering.

For this purpose, various investigation techniques have been used. ^{59}Co nuclear magnetic resonance (NMR) is a local probe of the short range structure and of the chemical environment around the Co atoms. X-ray diffraction gives information about the crystalline quality of the layers. Transmission electron microscopy (TEM) gives complementary information on the crystalline quality and on the size of the crystallites. The resistivity in an external magnetic field and hysteresis loops at 4 K and room temperature are measured to check the impact of the structural differences on the amplitude of the magnetoresistance, the AF exchange coupling, and the magnetization distribution at the interfaces.

To minimize the effect of the deterioration of the structure of the samples when increasing the number of successive layers,[13,14] this paper is mostly devoted to the study of Co/Ru/Co sandwiches.

II. SAMPLE PREPARATION

The geometry of the samples is the following:

$$\text{Substrate}\backslash \text{Ru buffer}\backslash \text{Co}_{3\ \text{nm}}\backslash \text{Ru}_{t_{\text{Ru}}}\backslash \text{Co}_{3\ \text{nm}}\backslash \text{Ru}_{5\ \text{nm}}.$$

For the sputtered samples, the substrate is silicon oxide and the buffer is 5 nm thick. Thicker buffers do not give any improvement of the magnetic and resistivity properties. For the UHV grown samples, the substrate is mica and the buffer is 15 nm thick [thickness necessary to have a (0001) single crystal with a flat surface]. For both series, the thickness of the spacer (t_{Ru}) varies from 0.4 to 3.6 nm.

Additional samples have been grown by both techniques: (i) multilayers for the x-ray diffraction studies, and (ii) single Co layers (with identical substrates, buffers, and capping layers) with various thicknesses in order to investigate the magnetization reduction at the interfaces.

The UHV evaporated samples were grown[15] under the following conditions: the background pressure was better than 10^{-10} Torr, the single crystal and flat Ru buffer layer was deposited onto the mica at a temperature of 875 K. After cooling the substrate down to 270 K, Co and Ru layers were grown. The deposition rate was about 0.005 nm per second for both elements. The RHEED (reflection high energy electron diffraction) patterns obtained during the growth show a high crystalline quality with a (0001) hcp orientation of the Co and Ru layers. The growth of Co onto the Ru buffer layer follows a layer by layer mechanism for the first four Co atomic layers. For thicker Co layers, nucleation of Co islands appears on the surface. In contrast, it is from the beginning of the Ru deposition that the atoms tend to agglomerate, by thermal diffusion driven by surface free energies,[16] leading to a 3D epitaxial growth. RHEED scans over the surface show a large crystalline coherency of the surface.

The sputtering conditions were optimized to obtain a GMR ratio as large as possible. Ru was deposited by RF sputtering and Co by RF magnetron sputtering, both with argon as neutral gas. The base pressure was 3.10^{-7} Torr and the Ar pressure 10^{-2} Torr. The samples are rotating on a table and pass at each rotation in front of the sputtering target. The metals are thus only deposited on the substrate during a fraction of time. The resulting sputtering rates are 0.025 nm per second for Ru and 0.2 nm per second for Co.

III. DIFFRACTION STUDIES RESULTS

It is well known that the crystalline structure and the interface morphology of the samples are very sensitive to the growth conditions and influence the electronic properties of the multilayers.[17,18] The aim of this section is to study in detail the differences in crystallinity and interface quality between the UHV-grown and sputtered samples. The structure inside the layers has been studied by x-ray diffraction and TEM, and the interface morphology by zero field NMR.

The study of the crystalline quality of the UHV-grown Co/Ru samples has been performed on a Philips high resolution x-ray diffractometer with a parallel monochromatic Cu $K\alpha_1$ in reflection mode. All experiments were performed *ex situ* at room temperature. The curvature of the mica and the presence of steps impede small-angle reflectivity studies. To improve the sensitivity, multilayers have been used. Figure 1(a) presents an x-ray diffraction spectrum for the $[Co_{2.4\ nm}Ru_{1.2\ nm}]\times 33$ multilayer. The very narrow and intense peak at $\theta=22.3°$ comes from the mica substrate. The peak at $\theta=21.08°$ corresponds to the Ru buffer layer ($d_{[0002]}=0.2141$ nm).

The main superlattice peak is indexed SR_n and the satellites are SR_{n-2} and SR_{n-1}. The presence of these satellites indicates the good quality of the superlattice periodicity in the sample.[19,20] Their distance is related to the bilayer thickness and from their intensities it is possible to obtain some information on the interdiffusion at the interfaces.[21] The detailed analysis of those spectra is given elsewhere.[14,22] The

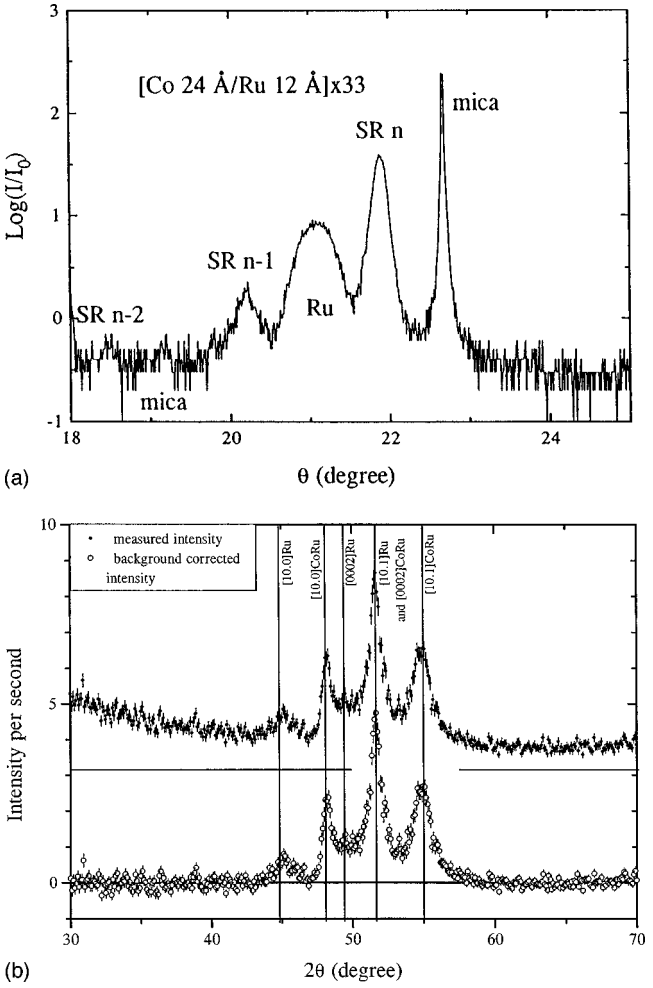

FIG. 1. X-ray diffraction spectra for the UHV-evaporated multilayer ($[Co_{2.4\ nm}Ru_{1.2\ nm}]\times 33$) (a) and for the sputtered multilayer ($[Co_{3\ nm}Ru_{0.5\ nm}]\times 15$) (b).

results are the following: interdiffusion extending over 2.5 to 3 atomic planes at the interfaces, no detectable strain in the layers (each element has its bulk lattice parameters).

The perpendicular coherence length was determined from the full width at half maximum of the SR_n peak, using the Scherrer law. It varies from 20 to 30 nm and indicates the good crystalline quality of the samples in the growth direction as five to seven bilayers are coherent in average. The width of the rocking curves (W_{RC}) across SR_n is related to the in-plane crystalline coherence length and to the mosaicity of the single crystal. Since the value is close to that of the Ru buffer layer ($W_{RC}=1.6°$ for the buffer and $1.8° \leqslant W_{RC} \leqslant 3.0°$ for the Co/Ru multilayer), and since the Ru buffer layer has a large coherence in the plane,[23] we can deduce that the in-plane coherence length of the multilayers lies between 10 and 60 nm. Let us note that W_{RC} is small compared to the values obtained by other groups with different kinds of buffers deposited on substrates of the same material.[24,25] It means that our samples have a weak mosaicity and a good coherence in the plane.

Fig. 1(b) presents an x-ray diffraction spectrum obtained at high angles on a $[Co_{3\ nm}Ru_{0.5\ nm}]\times 15$ sputtered multilayer. The three peaks expected in a hcp powder (by increasing angles $[10\bar{1}0]$, [0002], and $[10\bar{1}1]$) are observed

for the Ru buffer layer as well as for the CoRu average layer (assuming Vegard's law for both a and c parameters of the hcp). Two comments have to be made about the line intensities. First, in the case of a perfect powder, the relative intensities of the different peaks are proportional to their multiplicity (6, 2, and 12, respectively). Second, if the Ru buffer layer and the Co/Ru multilayer had the same texture, the ratio between the corresponding peaks of the two contributions should be in the ratio $I_{\mathrm{CoRu}}/I_{\mathrm{Ru}}=0.4$, taking into account their thickness and x-ray diffraction form factors. Figure 1(b) shows that none of the line sets (multilayer and buffer layer lines) follows the relative intensities expected for a powder diffraction spectrum and that the ratio between the buffer layer lines and the multilayer lines is also different from the 0.4 expected ratio. Hence we can conclude that this sample is slightly textured but with a different texture in the Co/Ru layers and in the Ru buffer layer.

TEM observations have been performed in plane view geometry (electron beam parallel to the growth direction) on a high resolution analytical electron microscope TOPCON EM002B with a 200 kV operating voltage. They confirm the good crystallinity of the UHV-grown samples.[23] The selected-area electron diffraction patterns [Fig. 2(a)] of the $Co_{3\ nm}Ru_{2.8\ nm}Co_{3\ nm}$ sandwich confirm the single crystal epitaxy: the Co and Ru layers have a hcp structure with a [0001] growth direction. The double spots correspond to the scattering of Co and Ru layers relaxed to their bulk crystalline parameters. The other small peaks around the [0000] and $[10\bar{1}\,1]\ldots$ -type peaks are due to double diffraction (arrows).

A selected-area electron diffraction pattern of a sputtered $Co_{3\ nm}Ru_{1.05\ nm}Co_{3\ nm}$ sandwich is presented in Fig. 2(b) and compared to the expected radii for the different Bragg peaks of Ru and CoRu (assuming a Vegard's law for both a and c). It corresponds clearly to a polycrystal: it is composed of rings instead of spots, which would be expected for a single-crystal sample [Fig. 2(a)]. The rings are nearly continuous, indicating that the grain orientations are randomly distributed in the plane of the sample. The most intense rings correspond to in-plane $[10\bar{1}\,1]$ and $[10\bar{1}\,0]$ -type peaks of Ru showing the presence of a slight texture in the sample (but different from that of the multilayer measured by x-ray scattering). It is not surprising to see predominantly the Ru contributions as this sample is a bilayer with total thicknesses of CoRu and Ru equal to 7 nm and 10 nm, respectively, giving rise to a ratio of 0.25 between the intensities of the peaks corresponding to CoRu and Ru. On the TEM plane view images, grains with different orientations are observed with a typical size of 5–10 nm.

To conclude, the x-ray and TEM studies have shown that the main difference between the two kinds of samples lies in their crystallinity (texture, grain size, etc.).

IV. NUCLEAR MAGNETIC RESONANCE RESULTS

Zero field ^{59}Co NMR has been performed at 4.2 K with a broadband automated spectrometer. This technique is sensitive to the local symmetry and local chemical environment of the probed atom (Co).[17] Thus it gives an insight into the crystallographic structure of the Co layers and in the morphology of the Co/Ru interfaces. The main line corresponds

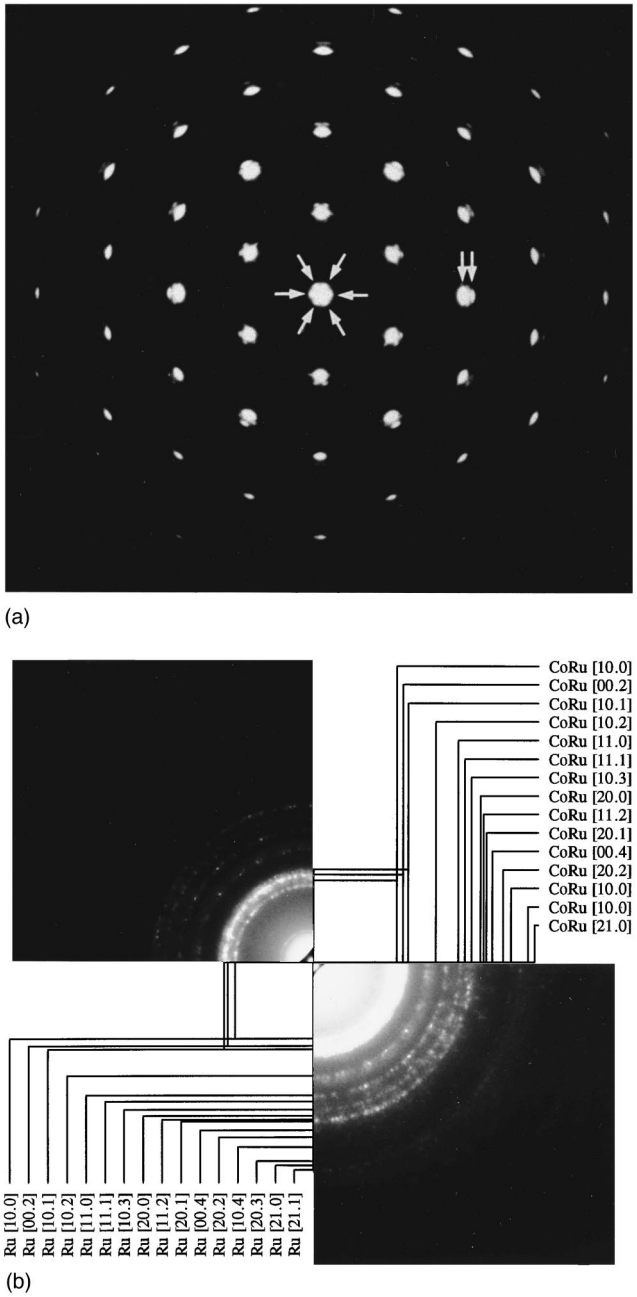

FIG. 2. Selected-area electron diffraction patterns of an UHV-evaporated Co/Ru sandwich ($Co_{3\ nm}Ru_{2.8\ nm}Co_{3\ nm}$) (a) and a sputtered sandwich ($Co_{3\ nm}Ru_{1.05\ nm}Co_{3\ nm}$) (b) (two printings of the same pattern).

to the Co atoms inside the Co layers. The frequency of this line is expected to lie between 225 and 228 MHz for a (0001) textured hcp sample with an in-plane magnetization and at 220 MHz for hcp Co with in-plane c axes and magnetization, whereas its frequency is close to 217 MHz in fcc samples.

Figure 3(a) shows the NMR spectra of UHV-grown and sputtered $Co_{3\ nm}Ru_{1.2\ nm}Co_{3\ nm}$ sandwiches. The main line resonance frequency is 224 MHz for the UHV-grown sample and 220 MHz for the sputtered one. Since 224 MHz is close to the expected resonance frequency for (0001) hcp Co, it confirms the good hcp stacking quality of the UHV sample already found by RHEED, x ray, and TEM. The 220 MHz

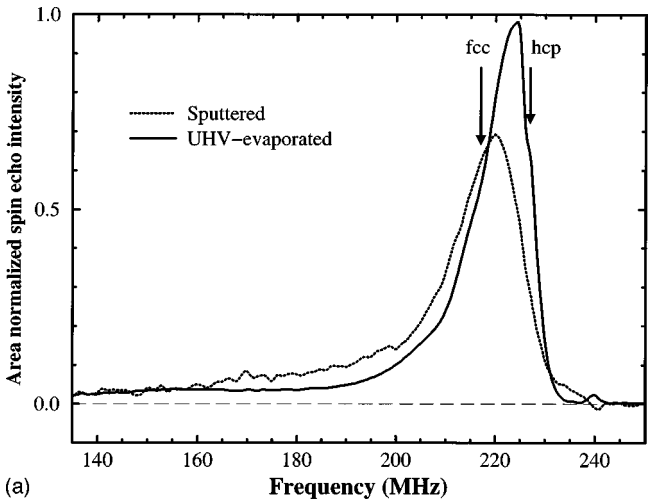

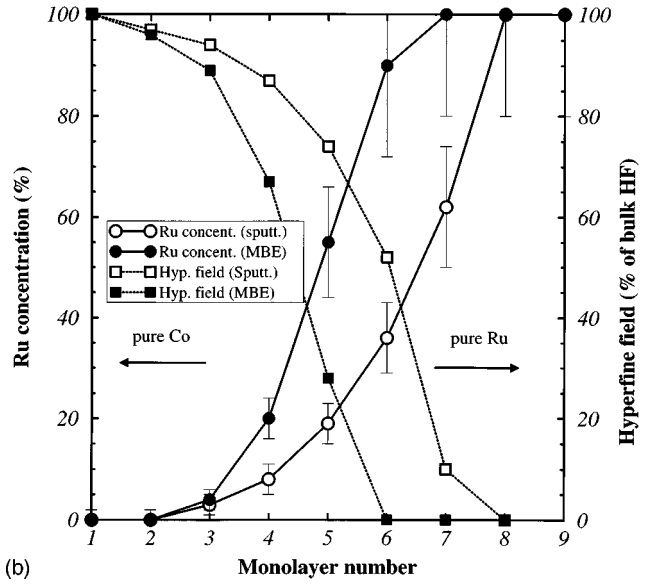

FIG. 3. NMR spectra (a) of UHV-grown and sputtered ($Co_{3\,nm}Ru_{1.2\,nm}Co_{3\,nm}$) sandwiches and the corresponding concentration profiles (b) across the interface, from pure Co to pure Ru.

main line resonance frequency observed for the sputtered sample can be explained on one hand by the absence of a well defined texture giving rise to a broad range of resonance frequencies, and on the other hand by the presence of stacking faults that generate locally a fcc structure. Since the two effects give rise to contributions in the same frequency range, it is not possible to favor one origin over the other.

The low frequency tail of the spectra arises from Co atoms with Ru atoms in their nearest neighbor shell,[17] i.e., Co atoms in the interfaces. The diffuse interface model already described in Refs. 17 and 26 enables a fit of the spectra and calculation of the Ru concentration profile in the interfaces. In Fig. 3(b) the layer number 2 corresponds to the pure Co atomic layer in contact with the first mixed one. The profiles in Fig. 3(b) show that there is a significant Co-Ru mixing at the interfaces for both samples. It has to be noted that in the case of such a large mixing, the shape of the interface spectra is not affected by the texture of the sample. The observed mixing is more important in the case of the sputtered sample: it extends over three atomic layers in the UHV-grown sample (in good agreement with the x-ray results) and over

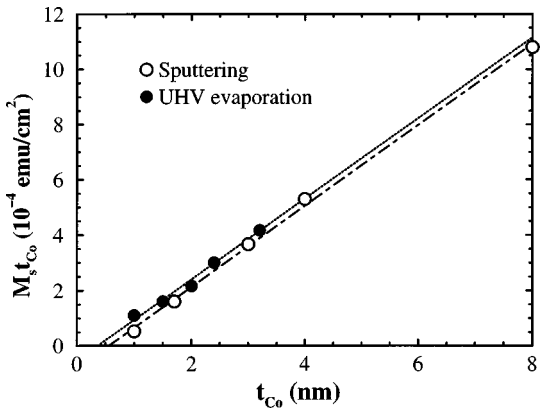

FIG. 4. Variation of the saturation magnetization per surface unit ($M_S . t_{Co}$) as a function of the Co thickness for single Co layers prepared by sputtering and UHV evaporation.

four or five layers in the sputtered sample. The stronger mixing observed for the latter can be explained by the fact that the energy of the incident atoms is much larger in the case of the sputtering technique and may cause backsputtering and hence additional mixing.

From the contribution of each mixed atomic layer to the total spectrum it is possible to compute the average hyperfine field value of each layer, which provides an estimate of the average magnetic moment per Co atom in each mixed layer.[26] The hyperfine field (magnetization) profiles, normalized to the bulk hyperfine field (bulk magnetization), are displayed as squares in Fig. 3(b). We find that the Co atoms in atomic layers containing more than 60% of Ru are no longer magnetic.

If we express the former concentration profiles in terms of magnetic dead layers per interface, we find 0.16 nm and 0.21 nm, respectively. This can be compared to the amount of magnetic dead layers deduced from the plot of the saturation magnetization versus the Co thickness (Fig. 4): 0.2 nm and 0.25 nm per interface for the UHV-grown and sputtered samples, respectively. Since the NMR spectra have been recorded at 4.2 K and the magnetization curves at room temperature, and taking into account the error bars, the results obtained by both methods are in agreement. This last point will be discussed in more detail in the section dealing with the influence of the magnetism of the mixed layers on the coupling mechanism.

To conclude the structural comparison, one can say that the main difference between the Co/Ru samples grown by UHV and those grown by sputtering lies in the crystalline structure. Whatever the growth technique is, the Co/Ru interfaces are strongly mixed (more for the sputtered samples). The impact of those differences on the coupling and on the magnetoresistance will be described in the next section.

V. MAGNETISM AND TRANSPORT: RESULTS AND DISCUSSION

In this section we first describe briefly the experimental procedure, then we present the results and the discussion of the measurements performed at room temperature. The last part of this section will be devoted to the study of the magnetization temperature dependence in a sputtered sample

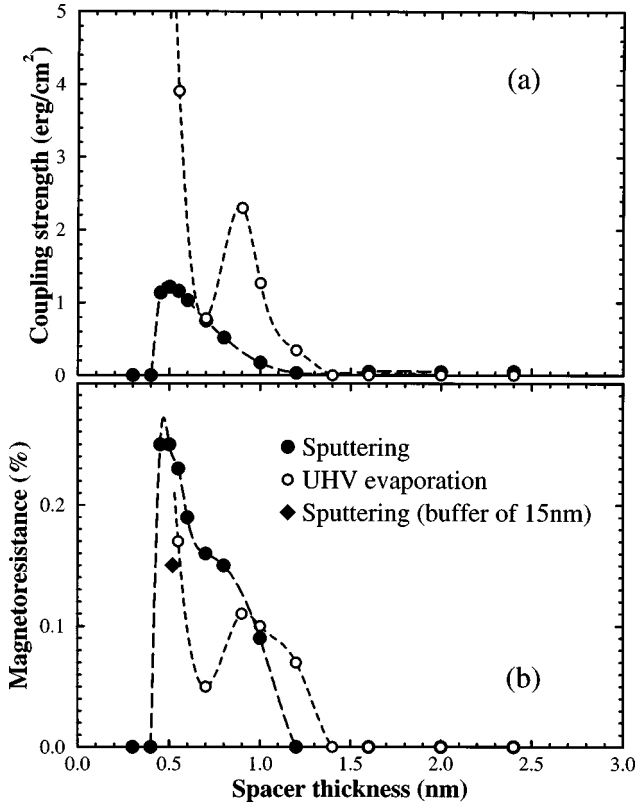

FIG. 5. Variations of the exchange coupling (a) and of the GMR (b) as a function of the Ru spacer thickness (t_{Ru}) at room temperature, for the UHV-grown and sputtered samples.

with a thin Ru thickness. The resistivity was measured in a magnetic field using the usual four-point probe method and the GMR is defined as the ratio of the total resistivity change ΔR to the resistivity at saturation field R. No anisotropic magnetoresistance effect has been observed. The strength of the coupling is deduced from the saturation field (H_S) of the magnetization loops obtained with an alternating gradient force magnetometer (AGFM) or a vibrating sample magnetometer (VSM) on the basis of the simple relation: $J = -H_S M_S t_{Co}/2$ for sandwiches, where t_{Co} is the thickness of one Co layer and M_S is the bulk Co magnetization.

A. Room-temperature results

The Ru thickness dependence of the coupling strength and of the magnetoresistance is displayed in Figs. 5(a) and 5(b), respectively. As expected, the shape of the curves depends on the growth conditions. The UHV-grown samples exhibit a minimum in the coupling strength at 0.7 nm (and correspondingly a GMR minimum), whereas the sputtered samples show broad coupling and GMR maxima with less defined structures. On average, the coupling strength is significantly bigger in the UHV-grown samples than in the sputtered samples. In contrast, the GMR ratios seem to be larger for the sputtered samples but the latter where grown with a Ru buffer layer of 5 nm instead of 15 nm for the UHV samples. In order to compare accurately the GMR values of the two series, an extra sample has been sputtered with a 15 nm buffer thickness and $t_{Ru}=0.5$ nm. The GMR signal (0.15%) measured in this sample [the diamond dot in Fig. 5(b)] is close to the value measured in the equivalent evaporated sample. The small remaining difference can be explained by the experimental error bars. Hence both series have comparable magnetoresistances.

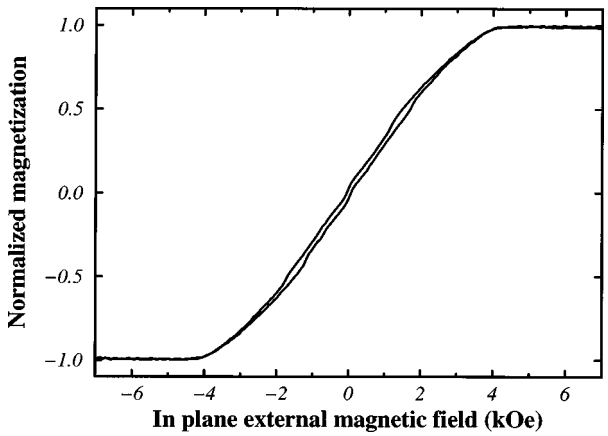

FIG. 6. Magnetization loop of the sputtered sandwich having a 0.6-nm-thick Ru spacer layer.

The first remark which can be made about these results is that, as already reported in the literature, the GMR is surprisingly small notwithstanding the large spin diffusion asymmetry (0.22) expected for the Co/Ru system.[12] An equivalent comment can be made about the coupling strength. Indeed, even if the observed coupling strength is much bigger than that obtained for many other multilayer systems, it is still one order of magnitude smaller than the theoretical values[27] (2.4 erg/cm^2 compared to 36 erg/cm^2 at $t_{Ru}=9$ nm). Even if the possibility of an overestimate of the computed value cannot be fully ruled out, it has to be noted that a recent study, similar to the present one, on the Co/Rh system gave very close agreement between the experimental and theoretical coupling values.[28] Since the NMR study has shown that the interfaces are strongly mixed independent of the growth technique (over three atomic layers for the UHV-grown samples and five atomic layers for the sputtered samples), both experimental observations (weak GMR and weak coupling compared to the theoretical results) find their origin in the bad quality of the Co/Ru interfaces. Indeed, the mixed region will affect the transport properties as well as the coupling strength. First the GMR effect is strongly reduced due to the strong mixing and the related magnetization reduction of the Co atoms at the Co/Ru interfaces, as described by the NMR hyperfine field profile, will strongly enhance the rate of spin-flip scattering.[29] Second, the effect of the interface diffusion on the value of the coupling strength can be explained in the framework of the theory describing the interlayer exchange coupling in terms of quantum interferences due to electronic confinement in the spacer layer.[9] The strength of the coupling is thus related to the reflection amplitudes for electron scattering at the interfaces between the spacer layers and the magnetic layers.[30] An extended interface reduces the confinement and hence weakens the coupling. Moreover, the presence of a significant number of intermixed layers at the interfaces gives rise to a progressive decrease of the magnetization from the Co layer to the Ru layer. Thus, the polarization of the conduction electrons within the spacer layer is reduced, which reduces the coupling. This interfacial mixing is intrinsic to this system as

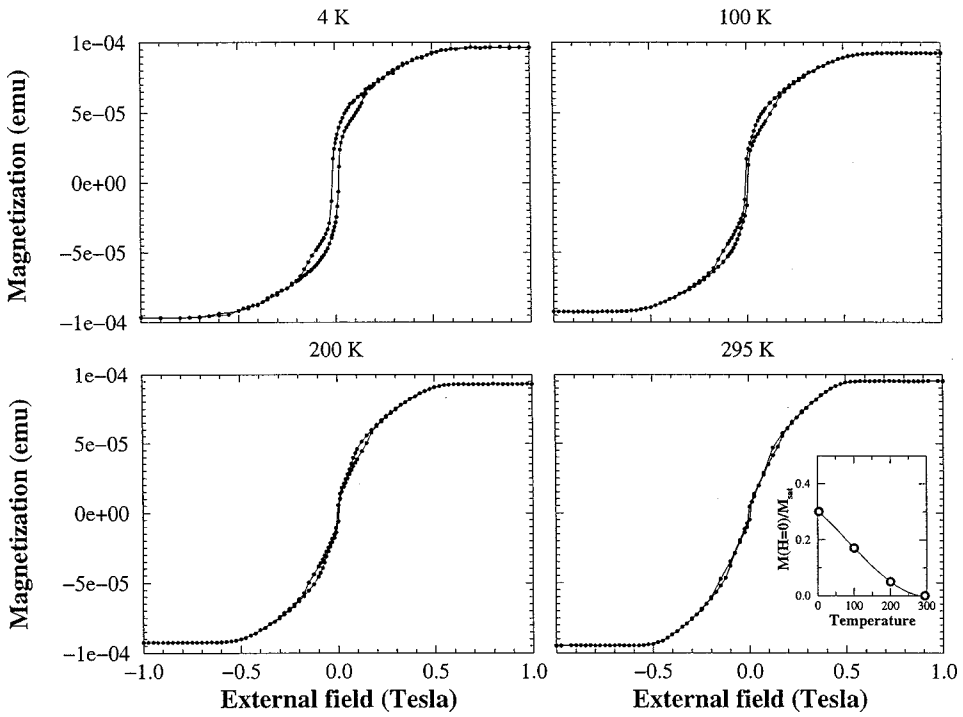

FIG. 7. SQUID magnetization loops on the sputtered sandwich having a thin spacer layer ($Co_{3\,nm}Ru_{0.5\,nm}Co_{3\,nm}$) at 4.2, 100, 200, and 300 K.

due to the total miscibility of Co and Ru over the whole concentration range [31] and will appear with any growth technique. Attempting to grow these multilayers at lower temperature,[15] epitaxial growth was no longer obtained. Thus, it seems impossible to get a strong GMR effect and a larger coupling strength in the Co/Ru system, unless the interface quality is significantly improved.

Compared to the UHV-grown samples, the coupling strength of the sputtered samples is even smaller. Our knowledge about the coupling mechanisms is not thorough enough to distinguish whether it originates from the extra interfacial mixing observed in those samples compared to the UHV samples or from the absence of a well defined texture.

A more detailed analysis of the shape of the coupling curves adds more information about the coupling mechanism. For both types of samples, there is an antiferromagnetic coupling (and a GMR signal) for t_{Ru} ranging from 0.4 to 1.2 nm, with a local AF coupling minimum for $t_{Ru}=0.7$ nm for the UHV-prepared samples. The *ab initio* calculations done by Stoeffler and Gautier[27] predict a ferromagnetic coupling when the spacer is three atomic layers thick. Experimentally, there is no ferromagnetic coupling but only a reduced AF coupling because of the intermixing between Co and Ru: the thickness of the spacer is not uniform in a scale below the lateral magnetic coherence length of the Co layers and the average coupling is on the AF side. The observation of the AF minimum at 0.7 nm, in agreement with the theoretical prediction of a ferromagnetic coupling, has been possible only because of the good crystallographic quality of the samples. In opposition, the sputtered samples do not present such a reduction of the coupling for 0.7 nm (only a slight reduction of the GMR is observed), because of their polycrystalline nature. Indeed several authors[9,30] have shown that the strength and phase of the coupling depend on the growth direction and therefore on the geometry of the Fermi surface and, as a consequence, are very sensitive to the structural quality of the samples. Hence, in the sputtered samples the coupling is laterally even more inhomogeneous and the smoothing tendency, already mentioned for the UHV samples, is enhanced.

The last comment about the room-temperature magnetotransport measurements concerns the thickness below which the AF coupling disappears and becomes ferromagnetic. Indeed, whereas the *ab initio* calculations[27] predict that the coupling should be AF and maximum for the thinnest spacer (one monolayer), experimentally, because of roughness, the exchange coupling is always ferromagnetic below some critical thickness. For the samples studied here, the coupling maxima are obtained for the same Ru thickness (0.5 nm), which is slightly larger than the values reported by other authors [0.4 nm (Ref. 11) and 0.3 nm (Ref. 2)]. The homogeneity of the coupling, even at such small Ru thickness, is still very good since their room-temperature magnetization loops do not present any remanence even for the thinnest spacers (about two atomic layers). Several studies have shown the presence of large remanence for very thin spacer layers (about two atomic layers) and have attributed this remanence to the presence of bridges between ferromagnetic layers. In our case the absence of the remanence at 0.5 nm Ru spacer layer at room temperature is the signature of a good homogeneity of the coupling. Furthermore, the magnetization loop of the sample having a 0.6-nm-thick spacer presents a perfect linear increase of the magnetization before saturation (Fig. 6), showing that the coupling is laterally homogeneous at a scale larger than the magnetic coherence length of the Co layers.[32] If we assume that the Co and Ru are intermixed, as determined by the NMR measurements, this sample with a 0.6 nm nominal thickness of spacer layer should not have any pure Ru atomic layer left, and the atomic layer richest in Ru should be still weakly magnetic.

Hence if we rely on the hyperfine field (magnetization) profile, this sample should be ferromagnetic.

B. Temperature dependence of the magnetization

Temperature-dependent SQUID magnetometry have been performed on the sputtered sandwich having the thinnest spacer layer and the strongest AF coupling ($Co_{3\ nm}Ru_{0.5\ nm}Co_{3\ nm}$) to explain the apparent inconsistency between the magnetization measurements and the concentration and magnetization profiles determined by NMR. The magnetization curves obtained at 4.2, 100, 200, and 300 K are presented in the Fig. 7. It can be observed that the remanence increases progressively with decreasing temperature (see the inset). This can only be explained by an enhancement of the magnetism of the interfaces causing the appearance of ferromagnetic bridges between the Co layers. This confirms the accuracy of the magnetization profiles determined by NMR at 4.2 K and shows that the layers which are still weakly magnetic at 4.2 K become nonmagnetic at room temperature. Hence at room temperature, there is still a nonmagnetic spacer in this sample. In other words, the effective nonferromagnetic spacer is larger (about two atomic layers) at room temperature than at 4.2 K and prevents any ferromagnetic bridge to appear between the Co layers. This set of results explains the persistence, at room temperature, of an AF coupling without any remanence for spacer thickness down to 0.5 nm in the sputtered sandwiches.

VI. CONCLUSION

This study sheds some light on the discrepancies noticed in the literature about the Co/Ru multilayers. We confirm the small GMR magnitude and suggest that it is mainly due to interfacial mixing. The AF coupling has been shown to be very sensitive to the crystalline quality. Indeed, only the samples grown by UHV evaporation present coupling oscillations in agreement with *ab initio* calculations. A more original result is obtained by the temperature-dependent magnetization measurements: the same interfacial mixing, at the origin of the small GMR, prevents, for low Ru thickness and at room temperature, the appearance of ferromagnetic bridges between the Co layers. However, the detailed influence of the interfacial mixing on the coupling strength is still not clearly understood. Further studies on samples with controlled interfacial mixing are in progress.

*Author to whom correspondence should be addressed. FAX: +333.88.10.72.49. Electronic address: aziz@atlas.u-strasbg.fr

[1] A. Fert, P. Grünberg, A. Barthélémy, F. Petroff, and W. Zinn, J. Magn. Magn. Mater. **140-144**, 1 (1995).
[2] S. S. P. Parkin, N. More, and K. P. Roche, Phys. Rev. Lett. **64**, 2304 (1990).
[3] B. Dieny, J. Magn. Magn. Mater. **136**, 335 (1994).
[4] G. Binasch, P. Grünberg, F. Saurenbach, and W. Zinn, Phys. Rev. B **39**, 4828 (1989).
[5] G. Rupp and K. Schuster, J. Magn. Magn. Mater. **121**, 416 (1993).
[6] M. T. Johnson, R. Coehoorn, J. J. de Vries, N. W. E. Mc Gee, J. Aan de Stegge, and P. J. H. Bloemen, Phys. Rev. Lett. **69**, 969 (1992).
[7] V. Grolier, D. Renard, B. Bartenlian, P. Beauvillain, C. Chappert, C. Dupas, J. Ferré, M. Galtier, E. Kolb, M. Mulloy, J. P. Renard, and P. Veillet, Phys. Rev. Lett. **71**, 3023 (1993).
[8] S. Araki, K. Yasul, and Y. Narumiya, Europ. patent Appl. 0504473A1 (1992).
[9] P. Bruno, Phys. Rev. B **52**, 411 (1995).
[10] K. Ounadjela, D. Muller, A. Dinia, A. Arbaoui, P. Panissod, and G. Suran, Phys. Rev. B **45**, 7768 (1992).
[11] P. J. H. Bloemen, H. W. van Kesteren, H. J. M. Swagten, and W. J. M. de Jonge, Phys. Rev. B **50**, 13 505 (1994).
[12] I. A. Campbell and A. Fert, in *Transport Properties of Ferromagnets*, Ferromagnetic Materials, edited by E. P. Wohlfarth (North-Holland, 1982), Vol. 3, Chap. 9.
[13] P. Panissod and C. Mény, J. Magn. Magn. Mater. **126**, 16 (1993).
[14] A. Michel, Ph.D. thesis, Louis Pasteur University, Strasbourg (1995).
[15] D. Muller, K. Ounadjela, P. Vennegues, V. Pierron-Bohnes, A. Arbaoui, J. P. Jay, A. Dinia, and P. Panissod, J. Magn. Magn. Mater. **104-107**, 1873 (1992).
[16] F. Gautier and D. Stoeffler, Surf. Sci. **249**, 265 (1991); F. Gautier and D. Stoeffler, in *Structural and Phase Stability of Alloys*, edited by J. M. Sanchez and J. L. Moran-Lopez *et al.* (Plenum Publishing Corporation, New York, 1991), pp. 181–197.
[17] P. Panissod, J. P. Jay, C. Mény, M. Wojcik, and E. Jedryka, Hyperfine Interact. **97/98**, 75 (1996).
[18] E. Petroff, A. Barthélémy, A. Hamzic, A. Fert, P. Etienne, S. Lequien, and G. Creuzet, J. Magn. Magn. Mater. **93**, 95 (1991).
[19] Y. Fujii, in *Metallic Superlattices*, Artificially Structured Materials, edited by T. Shinjo and T. Takada (Elsevier, Amsterdam, 1987), pp. 33–75.
[20] E. E. Fullerton, I. K. Schuller, H. Vanderstraeten, and Y. Bruynseraede, Phys. Rev. B **45**, 9292 (1992).
[21] W. Staiger, A. Michel, V. Pierron-Bohnes, N. Hermann, and M. C. Cadeville, J. Mater. Res. **12**, 161 (1997).
[22] J. P. Schillé, A. Michel, C. Mény, E. Beaurepaire, V. Pierron-Bohnes, and P. Panissod (unpublished).
[23] G. Z. Pan, A. Michel, V. Pierron-Bohnes, P. Vennegues, and M. C. Cadeville, J. Mater. Res. **10**, 1539 (1995); A. Michel, G. Z. Pan, V. Pierron-Bohnes, P. Vennegues, and M. C. Cadeville, J. Magn. Magn. Mater. **156**, 25 (1996).
[24] K. M. Krishnan, Y. Honda, Y. Hirayama, and M. Futamoto, Appl. Phys. Lett. **64**, 1499 (1994).
[25] H. A. M. de Gronckel, P. J. H. Bloemen, E. A. M. van Alphen, and W. J. M. de Jonge, Phys. Rev. B **49**, 11 327 (1994).
[26] Y. Henry, C. Mény, A. Dinia, and P. Panissod, Phys. Rev. B **47**, 15 037 (1993).
[27] D. Stoeffler and F. Gautier, J. Magn. Magn. Mater. **140-144**, 529 (1995).
[28] S. Zoll, A. Dinia, M. Gester, D. Stoeffler, J. P. Jay, and K. Ounadjela, Europhys. Lett. **39**, 323 (1997).
[29] A. Dinia and K. Ounadjela, J. Magn. Magn. Mater. **146**, 66 (1995).
[30] M. D. Stiles, Phys. Rev. B **48**, 7238 (1993).
[31] T. B. Massalski, in *Binary Alloy Phase Diagrams*, 2nd ed. (American Society of Metals, Metals Park, OH, 1990), Vol. 2.
[32] S. Zoll, H. A. M. Van den Berg, J. P. Jay, C. Meny, P. Panissod, D. Stoeffler, A. Dinia, and K. Ounadjela, J. Magn. Magn. Mater. **156**, 231 (1996).